Life Sciences 221 (2019) 109–120

Contents lists available at ScienceDirect

Life Sciences

journal homepage: www.elsevier.com/locate/lifescie

Telmisartan attenuates diabetic nephropathy progression by inhibiting the dimerization of angiotensin type-1 receptor and adiponectin receptor-1

Dongqing Zha, Tao Yao, Liping Bao, Ping Gao, Xiaoyan Wu*

Department of Nephrology, Zhongnan Hospital of Wuhan University, Wuhan, China

ARTICLE INFO

Keywords:
Telmisartan
Angiotensin II type 1 receptor
Adiponectin receptor 1
Diabetic nephropathy
Heterodimerization

ABSTRACT

Aims: The heterodimerization of angiotensin II receptors (AT1R and AT2R) with adiponectin receptor AdipoR1 and AdipoR2 may instigate high glucose (HG)-induced renal tubulointerstitial injury. This study examined the effect of telmisartan on diabetic nephropathy (DN) and its underlying mechanism.

Main methods: Diabetes was induced in rats through a single intraperitoneal injection of streptozotocin. Diabetic rats treated with or without the intravenous injection of AdipoR1 siRNA were intragastrically administered with 5 mg/kg/d telmisartan or a vehicle for 12 weeks. The rat proximal tubular epithelial cell line NRK-52E was treated with HG (30 mmol/L) with or without telmisartan (10 μM) for 48 h.

Key findings: In streptozotocin-induced diabetic rats, telmisartan treatment could decrease the inulin clearance rate, restore the glomerular surface area and mesangial area, alleviate renal fibrosis, and decrease urinary albumin excretion. Furthermore, diabetic rats exhibited increased AT1R-AdipoR1 heterodimers in the renal tubular compartment, which could be attenuated by telmisartan treatment, accompanied by a decrease in the expression level of cytokines MIP-1α, ICAM-1 and MCP-1. *In vitro*, HG promoted the dimerization formation of AT1R-AdipoR1 in cultured NRK-52E cells, but this effect was not found in NRK-52E cells transfected with the AdipoR1-G269E,G273E mutant. Telmisartan could inhibit HG-induced AT1R-AdipoR1 dimerization, down-regulate the expression levels of inflammatory cytokines, and alleviate cell apoptosis in NRK-52E cells. Furthermore, AdipoR1 knockdown could abate the renoprotective benefits of telmisartan.

Significance: The heterodimerization of AT1R-AdipoR1 probably contributes to the renal injury of DN, and provides an additional mechanistic insight into how telmisartan prevents the development and progression of DN.

1. Introduction

Diabetic nephropathy (DN) is one of the most threatening diseases worldwide, and is characterized by proteinuria and the progressive decline in renal function [1,2]. It has been reported that multiple factors are involved in the pathogenesis of DN, including the formation of advanced glycation end products, endoplasmic reticulum stress, the activation of protein kinase C, epigenetic regulations, oxidative stress, inflammation, the activation of fibroblasts, and lipid accumulation [3–8]. However, the molecular mechanisms leading to DN are multifactorial, complex, and not yet fully understood.

The activation of the renin angiotensin system, especially the angiotensin II (Ang II) type-1 receptor (AT1R) pathway, has been demonstrated to play a detrimental role in the progression of DN [9]. Adiponectin is an adipose tissue–derived secreted cytokine, which has insulin-sensitizing, anti-inflammatory and vasculoprotective actions through binding to its receptors, AdipoR1 and AdipoR2. These two adiponectin receptors have been previously shown to mediate the increase in AMPK activities, as well as the fatty acid oxidation and glucose uptake by adiponectin [10,11]. There is a growing body of evidence demonstrating the renoprotective functions of adiponectin and its receptors, which protects against the development of albuminuria [12–14]. In recent years, interactions between Ang II and adiponectin, as well as their receptors, have been investigated. Evidence has shown that adiponectin acts against Ang II-mediated inflammation and Ang II-accelerated atherosclerosis [15]. In addition, adiponectin attenuates Ang II-induced oxidative stress in renal tubular cells probably through the AMPK and cAMP-Epac signal transduction pathways [16].

The dimerization of receptors may influence receptor activation mechanisms and functional consequences [17]. The heterodimerization of receptors incurs a more profound biological significance, since it increases the complexity of cross-talk between different receptor

* Corresponding author at: Department of Nephrology, Zhongnan Hospital of Wuhan University, 169 Donghu Road, Wuhan, Hubei 430071, China.
E-mail addresses: wuxiaoyan2k6@163.com, wuxiaoyan2k6@whu.edu.cn (X. Wu).

https://doi.org/10.1016/j.lfs.2019.01.044
Received 29 August 2018; Received in revised form 25 January 2019; Accepted 26 January 2019
Available online 27 January 2019

systems. Receptor dimerization has been considered to play a role in the function of several members of the 7TM receptor family, including the GABA receptor, melanocortin receptor, and dopamine D2 receptor [18,19]. The disturbed dimerization has been implicated in several diseases, such as hypertensive cardiovascular disorders [20]. The previous *in vitro* experiments conducted by the investigators have revealed that high glucose induces the formation of differential heterodimers between Ang II receptors (AT1R and AT2R) and adiponectin receptors (AdipoR1 and AdipoR2) in renal tubular epithelial cells, contributing to renal tubular interstitial injury [21]. However, the determination of the kind of and manner on how adiponectin and Ang II receptors affect renal functions in DN, as well as the cross-talk of these two systems, remain unclear.

Telmisartan is an AT1R blocker that has been widely used to treat hypertension or other cardiovascular diseases. Aside from its blood pressure-lowering and cardioprotective actions, telmisartan exhibits beneficial effects against renal disease progression, and in particular, it has direct defensive action on diabetic kidneys [22]. Telmisartan has been known to have functions of anti-oxidative stress, anti-inflammation, and the inactivation of PPARγ-mediated insulin sensitization by blocking AT1R signaling in DN [23,24]. In addition, Ang II has been reported to inhibit the expression of cardiac AdipoR1 through the AT1R/ROS/ERK1/2/c-Myc pathway, while telmisartan upregulates the levels of myocardial adiponectin and AdipoR1 [25,26]. It was hypothesized that telmisartan might exert a renoprotective effect against DN through some unknown mechanisms, such as the interaction of AT1R and AdipoR1. The present study explored the effect of telmisartan on an early-stage DN rat model, and elucidated the possible molecular mechanisms through the crosstalk between AT1R and AdipoR1.

2. Materials and methods

2.1. Reagents

Mouse AT1 monoclonal antibody (ab9391), rabbit AdipoR1 monoclonal antibody (ab126611), mouse intercellular cell adhesion molecule (ICAM) monoclonal antibody (ab171123), and rabbit α-smooth muscle actin (α-SMA) polyclonal antibody (ab5694) were purchased from Abcam (Cambridge, MA, USA). Rabbit monocyte chemoattractant protein-1 (MCP-1) polyclonal antibody (sc-28879), rabbit AT1 polyclonal antibody (sc-579), goat AdipoR1 polyclonal antibody (sc-46748), mouse macrophage inflammatory protein-1α (MIP-1α) monoclonal antibody (sc-365691), and AdipoR1 siRNA (sc-156024) were purchased from Santa Cruz Biotechnology (Santa Cruz, CA, USA). Rabbit nuclear factor-kappa B (NF-κB) monoclonal antibody (#8242), rabbit monoclonal phospho-AMPK antibody (#2535), and rabbit monoclonal AMPK antibody (#5832) were obtained from Cell Signaling Technology (Danvers, MA, USA). Mouse β-actin monoclonal antibody (A5316), streptozotocin (STZ, S0130), G418 (PP2374), and telmisartan (T8949) were purchased from Sigma-Aldrich (St. Louis, MO, USA). Rabbit fibronectin monoclonal antibody (NBP1-91258) was purchased from NOVUS Biologicals (Littleton, CO, USA). The Albuwell M Test kit (#1011) was purchased from Exocell Inc. (Philadelphia, PA, USA). The QuantiChrom™ Creatinine Assay Kit (#DICT-500) was purchased from BioAssay System (Hayward, CA). Inulin (FIT-0408) and the inulin EIA kit (FIT-0415) were purchased from BioPhysics Assay Laboratory (BioPAL; Worcester, MA, USA). The Annexin-FITC Apoptosis Detection Kit was purchased from BD Bioscience (San Diego, CA, USA). The X-tremeGENE HP DNA Transfection Reagent was purchased from Roche (Basel, Switzerland). Angiotensin II was purchased from Enzo Life Science (Netherlands).

2.2. Animals

A total of 60 male specific pathogen-free Wistar rats (200–220 g of body weight, eight weeks old) were obtained from the Hubei Research Center of Experimental Animals, the Disease Prevention and Control Centers of Hubei Province, China. These rats were randomly divided into three groups: control group, diabetic mellitus (DM) group, and DM + telmisartan group. Diabetes was induced in rats through a single intraperitoneal injection of STZ (60 mg/kg). Rats with blood glucose > 16.67 mmol/L were deemed to have developed DM. Natrium citricum buffer solution of the same volume were intraperitoneally injected in rats in the control group. The diabetic rats were treated with or without the intravenous injection of AdipoR1 siRNA (50 nmol, three days), followed by intragastric administration with telmisartan (5 mg/kg/d) or distilled water (vehicle) for 12 weeks. Blood and urine samples were collected before rats were sacrificed after 12 weeks.

The present study was conducted according to the Guide for the Care and Use of Laboratory Animals [27], and was approved by the Animal Ethics Committee of Wuhan University.

2.3. Measurement of albuminuria

Urinary albumin was measured using a murine microalbuminuria ELISA kit. Urinary creatinine was determined using a QuantiChrom™ Creatinine Assay Kit. Urinary albumin and creatinine were analyzed using SoftMax pro 6.4 (Molecular Devices, Sunnyvale, CA, USA).

2.4. Inulin clearance rate

All rats were intraperitoneally injected with 0.5 ml/kg of inulin before sacrifice. Serum or urinary inulin was measured using an inulin EIA kit, according to manufacturer's instructions. Blood and urinary inulin concentrations were analyzed using SoftMax pro 6.4. The inulin clearance rate was calculated using the formula: urinary inulin concentration × 24-hour urinary volume / serum inulin concentration.

2.5. Histopathology

The kidney was fixed in 10% formaldehyde and embedded in paraffin. The deparaffinized sections were stained with periodic acid-Schiff (PAS), or Masson's trichrome or Picrosirius red. The glomerular surface area was calculated in 10 PAS-stained glomeruli from each rat using ImageJ software (Research Services Branch, NIH, USA). Ten randomly selected Masson's trichrome-stained or Picrosirius red-stained visual areas per rat were analyzed, and the fibrotic area of the analyzed field was measured using ImageJ software.

2.6. Immunohistochemistry

The paraffin-embedded sections of kidney tissues were deparaffinized and dehydrated, followed by microwave antigen retrieval for five minutes. After peroxidase quenching with 3% H_2O_2 in phosphate-buffered saline (PBS) for 15 min, the sections were blocked with 5% bovine serum albumin (BSA) for 30 min, and incubated with primary antibodies (1:100) overnight at 4 °C. After washing in PBS for three times, the sections were incubated with biotinylated secondary antibodies for 30 min, and stained with 3,3′-diaminobenzidine (DAB) for three minutes. After counterstaining with hematoxylin for 2–3 min, the sections were mounted and analyzed.

2.7. Double-label immunofluorescence

The frozen sections were fixed in 4% formaldehyde for 20 min at room temperature. After blocking with 5% BSA for 30 min, the sections were incubated with mouse AT1 monoclonal antibody (1:100) and rabbit adipoR1 monoclonal antibody (1:100) overnight at 4 °C. Then, the sections were re-warmed for 45 min at 37 °C, and incubated with Cy^3-labbeled goat anti-mouse IgG or FITC-conjugated goat anti-rabbit IgG for 90 min, respectively. The immunological reactions were imaged by fluorescence microscopy (BX53TR-32FB3F0, OLYMPUS Corporation,

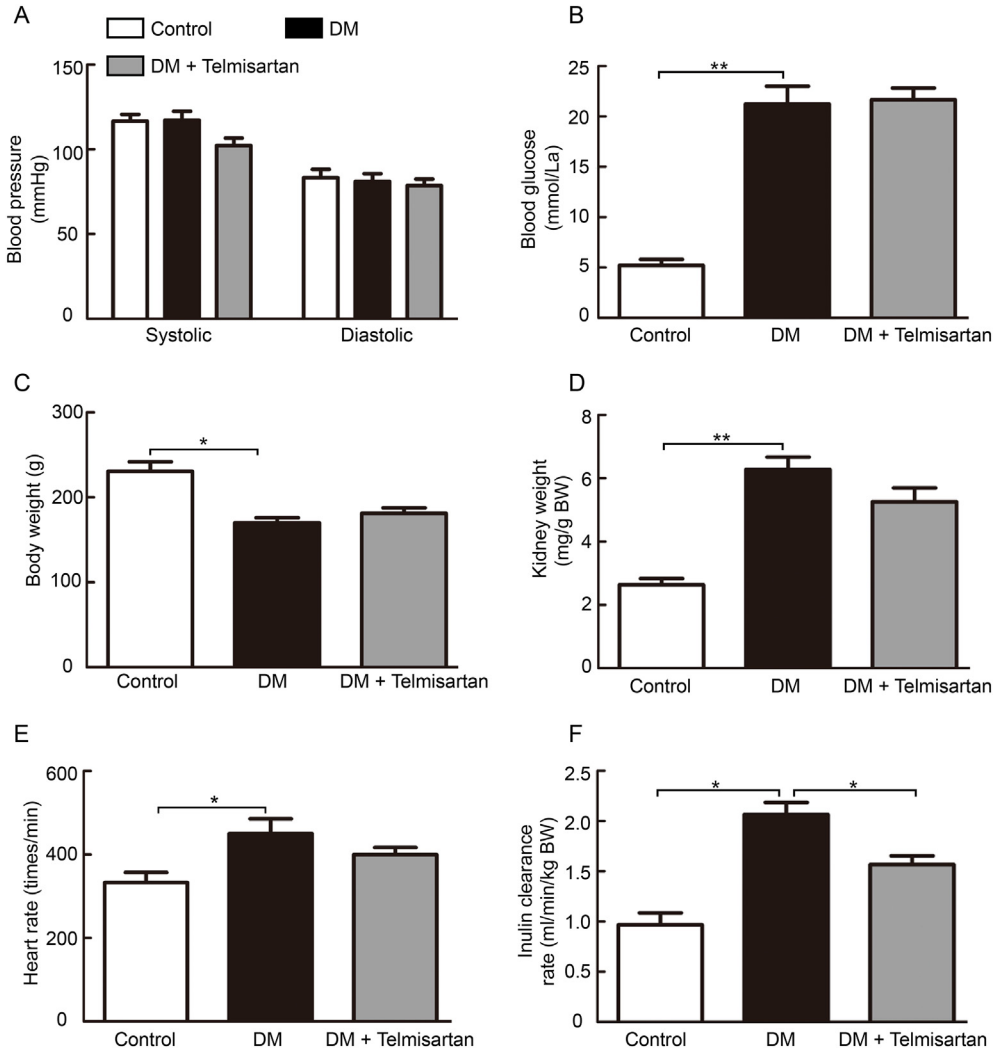

Fig. 1. Effect of telmisartan on physical and biochemical parameters: (A) Systolic and diastolic blood pressure; (B) Blood glucose; (C) Body weight; (D) Kidney weight (per gram of body weight); (E) Heart rate; (F) Inulin clearance rate. Data were expressed as mean ± standard error of the mean (SEM); $n = 5$ in each group; $^{*}P < 0.05$, $^{**}P < 0.001$.

Japan).

2.8. Cell culture and treatment

The rat proximal tubular epithelial cell line (NRK-52E) was purchased from the Shanghai Academy Cell Bank, China. NRK-52E cells were cultured in DMEM medium (Gibco, Grand Island, NY, USA), supplemented with 10% fetal calf serum (Gibco) and 100 U/ml of penicillin/streptomycin, in an incubator with 5% CO_2 at 37 °C. Cells at passages 15–20 were used. The cultured cells were treated with high glucose (30 mmol/L) with or without telmisartan (10 μM) for 48 h.

Human renal tubular epithelial cell line (HK-2) cells (CRL-2190™; ATCC) were cultured in Keratinocyte Serum Free Medium (K-SFM; Cat# 17005-042, Invitrogen, Carlsbad, CA, USA), supplemented with 0.05 mg/ml of bovine pituitary extract (BPE) and 5 ng/ml of human recombinant epidermal growth factor. Then, these cultured cells were treated with high glucose (30 mmol/L) with or without telmisartan (10 μM) for 48 h.

2.9. Transfection

The pcDNA3.1-AT1R was constructed by Wuhan Biofavor Biotechnology, China. The transfection of the AT1R plasmid was performed using the X-tremeGENE HP DNA Transfection Reagent, according to manufacturer's instructions. Briefly, 6×10^5 cells were seeded in a 100-mm dish, and incubated with transfection complexes containing 4, 8 and 12 μg of AT1R plasmid or a vector, and 15 μl of X-tremeGENE transfection reagent for 72 h. G418 (Sigma-Aldrich) was used for the selection of stably-transfected cells.

NRK-52E cells were transfected with complexes containing the AdipoR1-G269E,G273E mutant or control vector for 48 h at 37 °C. The AdipoR1-G269E,G273E mutant transfection was performed using the X-tremeGENE HP DNA transfection reagent (Roche, Basel, Switzerland), according to manufacturer's instructions.

AdipoR1 siRNA was transfected according to the Santa Cruz transfection reagent handbook. Briefly, 6×10^5 cells were seeded in a 100-mm dish and transfected with 20 nM of AdipoR1 siRNA or a scrambled siRNA (negative control). Then, cells were incubated with the transfection complexes at 37 °C for 48 h.

2.10. Confocal microscopy

After washing twice with PBS, NRK-52E cells were fixed in methanol for 10 min and cold acetone for one minute at −20 °C. Then, cells were blocked with 2% BSA in PBS, and incubated with mouse AT1 monoclonal antibody (1:100) and rabbit adipoR1 monoclonal antibody

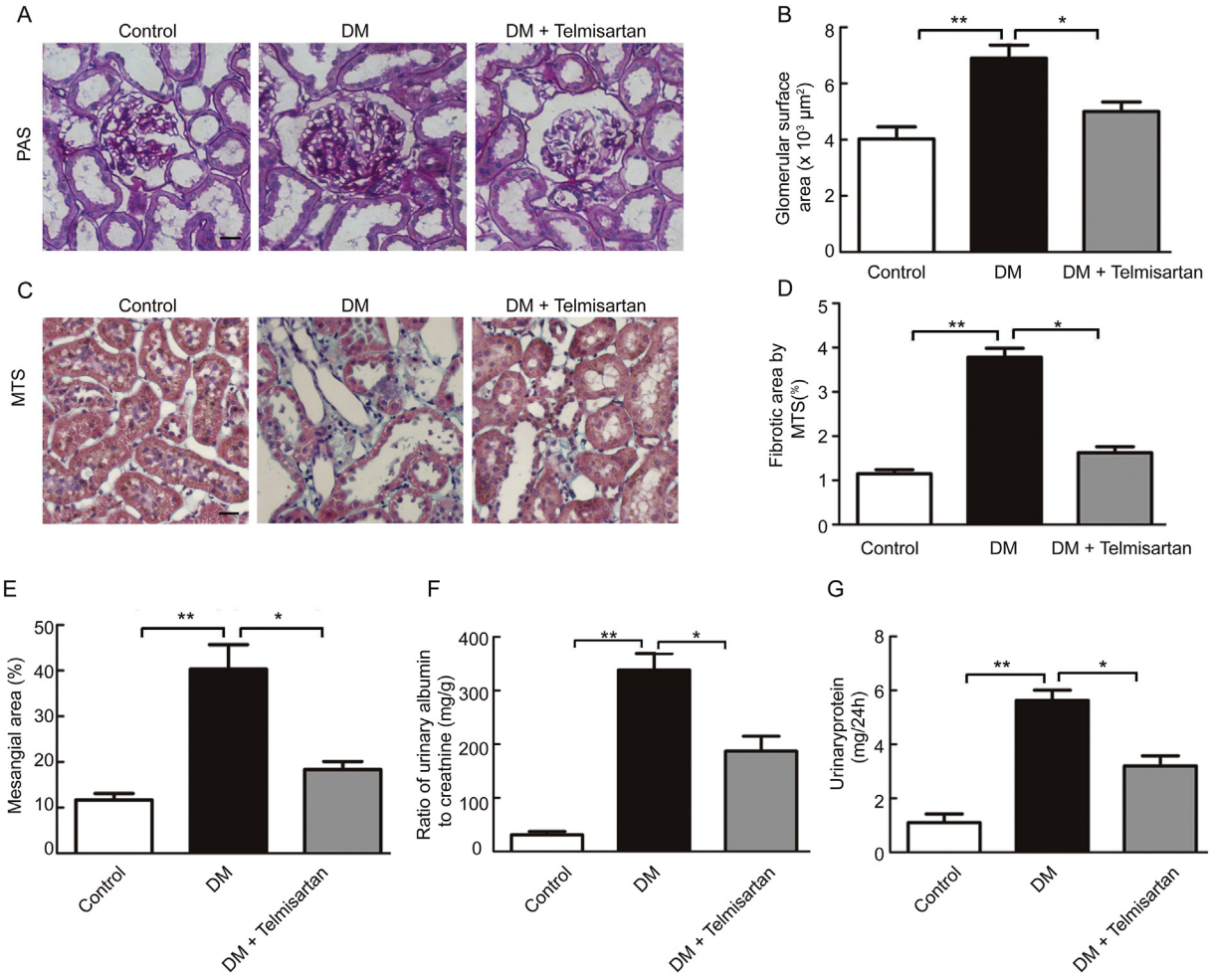

Fig. 2. Effect of telmisartan on STZ-induced diabetic rats. (A) Periodic Acid-Schiff staining of glomeruli in the indicated groups; Original magnification, ×400; Scale bar = 50 μm. (B) Quantification of the glomerular surface area. Ten glomeruli from each rat were analyzed to calculate the glomerular surface area using ImageJ software. (C) Masson's trichrome staining (MTS) of kidneys in the indicated groups; Original magnification, ×400; Scale bar = 50 μm. (D) Quantification of the relative fibrotic area by MTS. A total of 10 Masson's trichrome-stained visual areas were analyzed from each rat to calculate the fibrotic area using ImageJ software. (E) Quantification of the mesangial area in the indicated groups. A total of 10 glomeruli were analyzed from each rat to calculate the glomerular surface area using ImageJ software. (F) Urinary albumin excretion was analyzed using the albumin/creatinine ratio. (G) Quantification of 24-hour urinary protein in the indicated groups. Data were expressed as mean ± standard error of the mean (SEM); $n = 5$ in each group; $^{*}P < 0.05$, $^{**}P < 0.001$.

(1:100) overnight at 4 °C. The Cy^3-labeled goat anti-mouse IgG and FITC-conjugated goat anti-rabbit IgG secondary antibodies (1:200) were incubated for 30 min at room temperature. Then, the confocal sections were analyzed using the Openlab Confocal Imaging software (Improvision, Coventry, England).

2.11. Western blot

Kidney tissues and cells were lysed in lysis buffer (containing PMSF). The protein lysates were centrifuged at 13,000 rpm for 15 min at 4 °C. After centrifugation, bicinchonic acid (BCA) protein assay was used to assess the protein concentration in the supernatant. The lysate samples with Laemmli sample buffer were denatured by boiling at 95 °C for five minutes. Then, 20 μg of proteins were separated by 12% sodium dodecyl sulfate-polyacrylamide gels (SDS-PAGE), and transferred electrophoretically onto a nitrocellulose membrane. Next, the membranes were blocked in 5% skimmed milk and incubated overnight with the primary antibodies at 4 °C. Rabbit anti-MCP-1 (1:200), rabbit anti-NF-κB (1:1000), mouse anti-AT1 (1:200), goat anti-AdipoR1 (1:200), mouse anti-MIP-1α (1:200), rabbit anti-α-SMA (1:800), rabbit anti-fibronectin (1:500), mouse anti-ICAM (1:500), and mouse anti-β-actin (1:10000) were used as the primary antibodies. After washing with Tris-buffered saline (TBS) containing 0.05% Tween 20 (TBST), the membranes were incubated with the corresponding secondary antibodies for one hour. Immunoreactive bands were detected using the Super Signal enhanced chemiluminescence (ECL) system and LAS-4000 imaging system. The quantification of results obtained from the immunoblotting was analyzed by scanning densitometry.

2.12. Co-immunoprecipitation

Kidney tissues or cells were lysed in immunoprecipitation buffer and centrifuged at 15,000 rpm for 15 min at 4 °C. Then, the supernatant was mixed with rabbit IgG and protein A/G agarose for two hours at 4 °C, and centrifuged at 2500 rpm for five minutes. Afterwards, the supernatant was incubated with rabbit AT1 monoclonal antibody or rabbit AdipoR1 monoclonal antibody overnight at 4 °C, followed by mixing with protein A/G agarose for three hours to couple the antibodies to the protein A/G agarose. Next, the mixtures were centrifuged at 2500 rpm for five minutes. Then, the supernatant was discarded, and the precipitate was washed for five times with PBS. The complex was mixed with 1× Lane Marker Sample Buffer and heated at 100 °C for five minutes. Then, the samples were separated by SDS-PAGE and analyzed by immunoblotting with goat AdipoR1 and mouse AT1 antibodies,

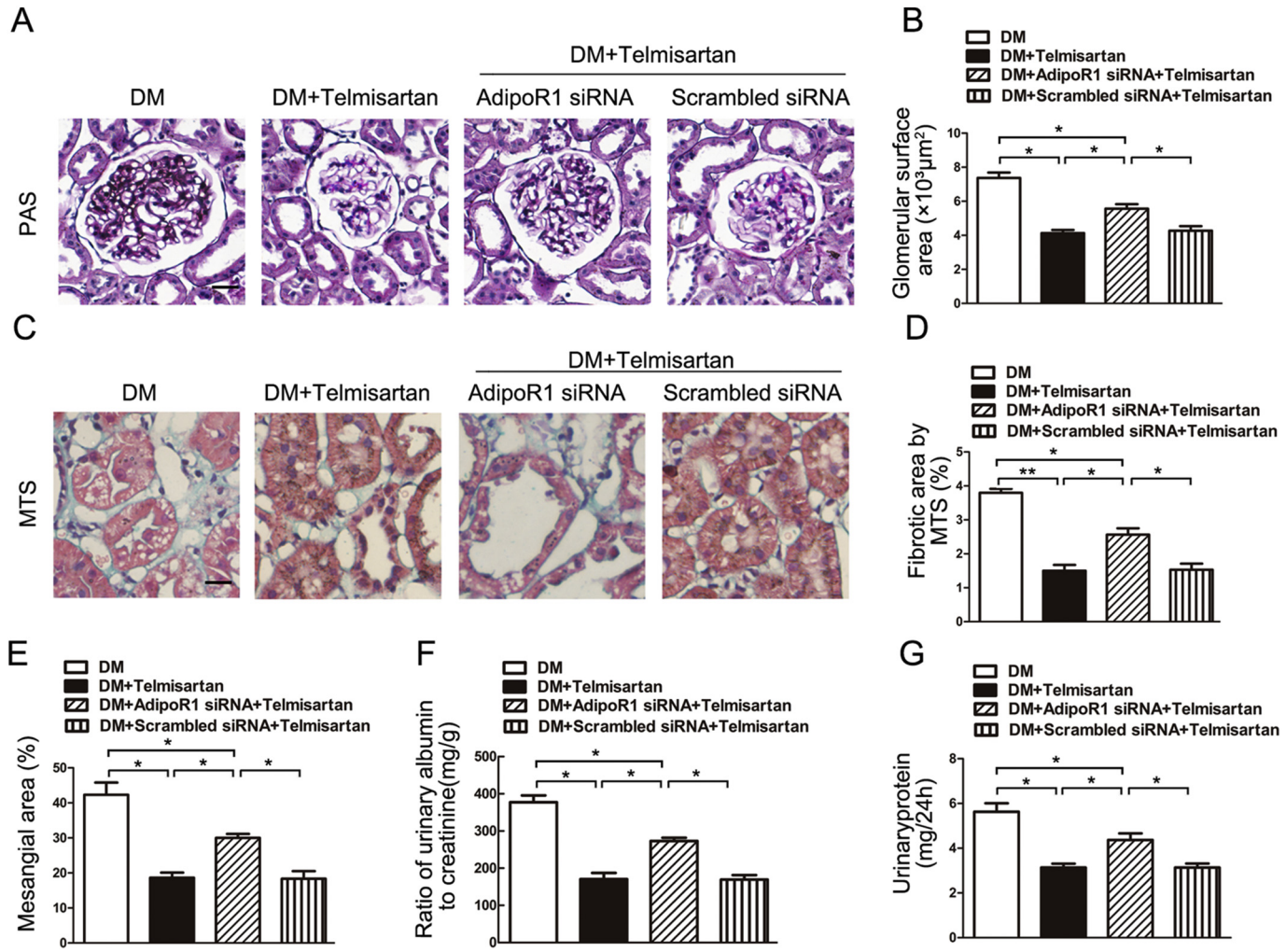

Fig. 3. The effect of telmisartan on streptozotocin-induced diabetic rats is dependent on AdipoR1. (A) Periodic Acid-Schiff staining of glomeruli in the indicated groups; Original magnification, ×400; Scale bar = 50 μm. (B) Quantification of the glomerular surface area. A total of 10 glomeruli were analyzed from each rat to calculate the glomerular surface area using ImageJ software. (C) Masson's trichrome staining (MTS) of kidney tissues in the indicated groups; Original magnification, ×400; Scale bar = 50 μm. (D) Quantification of the relative fibrotic area by MTS. A total of 10 Masson's trichrome-stained visual areas were analyzed from each rat to calculate the fibrotic area using ImageJ software. (E) Quantification of the mesangial area in the indicated groups. A total of 10 glomeruli were analyzed from each rat to calculate the mesangial area using ImageJ software. (F) Urinary albumin excretion was analyzed using the albumin/creatinine ratio. (G) Quantification of 24-hour urinary protein in the indicated groups. $^{*}P < 0.05$, $^{**}P < 0.001$.

respectively.

2.13. Flow cytometry

Cells were collected with 0.25% trypsin after washing for three times with PBS. The cell suspension was mixed with 1× binding buffer. The mixture was added with Annexin V-FITC and PI, and incubated for 10 min at room temperature. The cell apoptosis rate was detected by flow cytometry. The total of early apoptotic cells in the lower right quadrant and late apoptotic cells in the upper right quadrant were used for analysis.

2.14. Statistical analysis

All data were expressed as mean ± standard error of the mean (SEM). Statistical differences among groups were tested by one-way analysis of variance (ANOVA), followed by Tukey's HSD test. The differences were considered significant at $P < 0.05$. Statistical analyses were performed using the SPSS software (version 18.0; SPSS Inc., Chicago, IL, USA).

3. Results

3.1. The effect of telmisartan on physical and biochemical parameters

There was no difference in blood pressure between STZ-induced diabetic rats and control rats (Fig. 1A). Diabetic rats had significantly higher blood glucose, kidney weight (per gram of body weight), heart rate and inulin clearance rate, but had lower body weight, when compared with control rats (Fig. 1B–F). Telmisartan could decrease the inulin clearance rate in diabetic rats (Fig. 1F). However, there were no statistical differences between the DM group and DM + telmisartan group with regard to blood pressure, blood glucose, body weight, kidney weight and heart rate (Fig. 1A–E).

3.2. Telmisartan restored the histological changes in kidney tissues in STZ-induced diabetic rats

All rats were sacrificed at 12 weeks after the induction of diabetes. Diabetic rats exhibited an increased glomerular surface area and mesangial area by PAS staining, when compared with control rats. Telmisartan could restore the glomerular surface area and mesangial

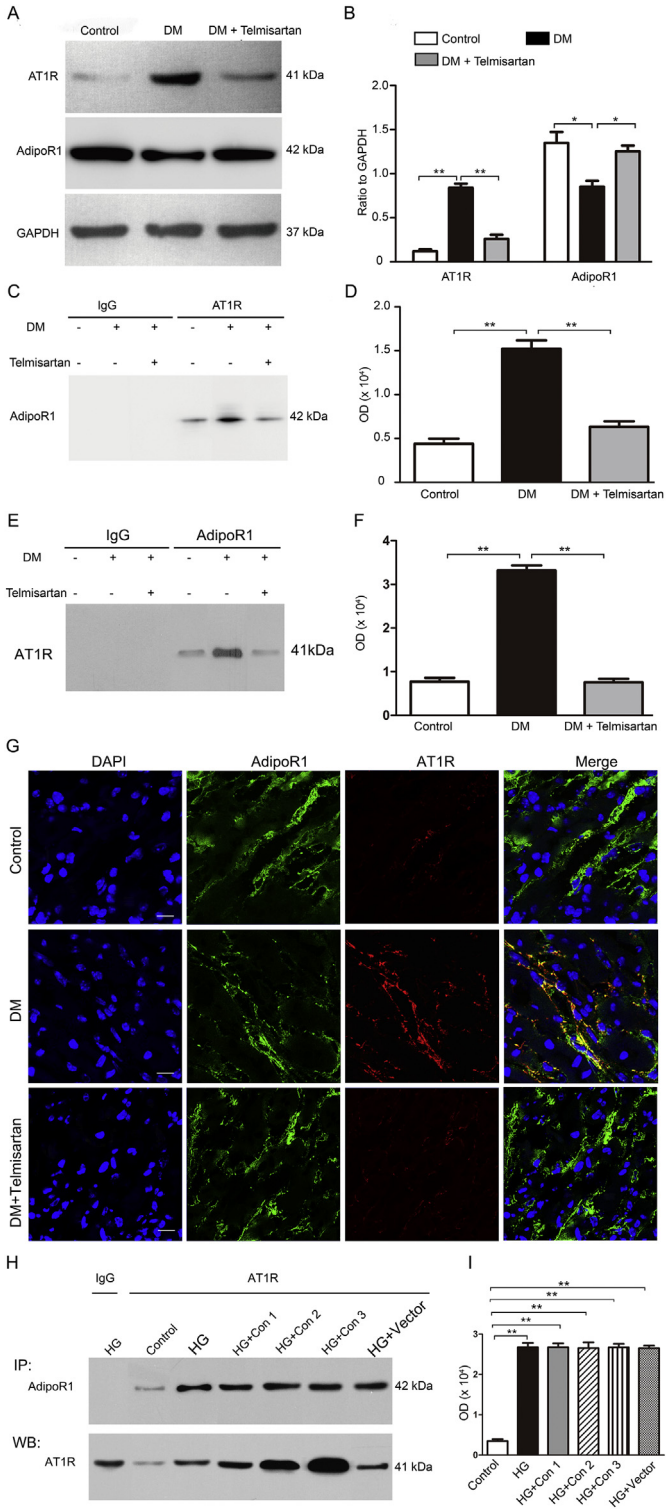

Fig. 4. Telmisartan inhibited the AT1R-AdipoR1 heterodimerization in diabetic kidneys. (A) Western blot analysis of AdipoR1 and AT1R expression in kidneys, and (B) the densitometry of the respective blots are shown. (C–F) The co-immunoprecipitation analysis of AT1R-AdipoR1 interaction in kidneys (C and E), and the densitometric analysis of the dimerization of AT1R-AdipoR1 (D and F) are presented. (G) Representative images of the co-expression of AT1R-AdipoR1 in the renal tubular compartment by confocal microscopy. Original magnification, ×630; Scale bar = 20 μm. (H) Co-immunoprecipitation analysis of AT1R-AdipoR1 interaction in cultured NRK-52E cells stimulated by high glucose (HG) with or without the different concentrations pcDNA3.1-AT1R plasmids (con1, 4 μg; con2, 8 μg; con3, 12 μg). (I) The densitometric analysis of the dimerization of AT1R-AdipoR1 is presented. $^{*}P < 0.05$, $^{**}P < 0.001$.

area in diabetic rats to a level similar to that of the control group (Fig. 2A, B and E). Similarly, diabetic rats displayed a greater fibrotic area by Masson trichrome staining, while telmisartan alleviated renal fibrosis in diabetic rats to a level comparable to the control group (Fig. 2C and D). In addition, diabetic rats exhibited a remarkable increase in urinary albumin/creatinine ratio, as well as 24-hour urinary protein, when compared to control rats. However, telmisartan was able to significantly decrease urinary protein in diabetic rats (Fig. 2F and G).

3.3. The effect of telmisartan on STZ-induced diabetic rats is dependent on AdipoR1

In order to determine whether the absence of AdipoR1 could attenuate the renoprotective effect of telmisartan, diabetic rats treated with the intraperitoneal injection of AdipoR1 siRNA were used. When compared with diabetic rats treated with telmisartan, rats with the knockdown of AdipoR1 had a larger glomerular surface area and mesangial area by PAS staining, as well as a greater fibrotic area by Masson trichrome staining (Fig. 3A–E). In addition, the knockdown of AdipoR1 resulted in a remarkable increase in 24-hour urinary protein, as well as urinary albumin/creatinine ratio (Fig. 3F–G). These data suggest that AdipoR1 knockdown could abate the renoprotective role of telmisartan.

3.4. Telmisartan inhibits AT1R-AdipoR1 heterodimerization

Western blot analysis revealed that AT1R expression increased and AdipoR1 expression decreased in diabetic kidney tissues (Fig. 4A and B). Furthermore, the co-immunoprecipitation analysis revealed the enhanced interaction of AdipoR1 and AT1R in diabetic kidneys (Fig. 4C–F). The expression and co-expression of AdipoR1 and AT1R in the renal tubular compartment was measured by confocal microscopy. The present results revealed that the expression of AdipoR1 remained unchanged, while the expression of AT1R, as well as the co-expression of AdipoR1 and AT1R, was enhanced in the renal tubular compartment of diabetic rats (Fig. 4G). In addition, the enhanced interaction of AdipoR1 and AT1R was independent of the increased expression of AT1R in cultured NRK-52E cells (Fig. 4H and I). These data are suggestive of the increased AT1R-AdipoR1 heterodimers in diabetic kidneys, especially in the renal tubular compartment. Interestingly, the treatment of telmisartan for 12 weeks attenuated the heterodimerization of AT1R-AdipoR1 in diabetic kidneys (Fig. 4C–G).

3.5. Telmisartan inhibits inflammation programming in diabetic kidneys

In parallel with the increased heterodimerization of AT1R-AdipoR1 in diabetic kidneys, diabetic rats had significantly higher levels of inflammatory cytokines, including MIP-1α (Fig. 5A and B), ICAM-1 (Fig. 5C and D), and MCP-1 (Fig. 5E and F), in kidneys by immunohistochemistry. In addition, telmisartan inhibited the expression of inflammatory cytokines MIP-1α, ICAM-1 and MCP-1 in diabetic kidneys (Fig. 5A–F).

3.6. The high glucose-induced heterodimerization of AT1R-AdipoR1 promotes cellular damage in cultured NRK-52E cells

Although the increased dimerization formation of AT1R-AdipoR1 in diabetic kidneys was found, its effects on DN remain unclear. It has been reported that AdipoR1 possesses a GxxxG dimerization motif, and the homodimerization and heterodimerization of AdipoR1 depends on a glycophorine-A-like dimerization motif in TMD5 [28]. Gly269 and Gly273 have been reported as key domains to produce the homodimers and heterodimers of AdipoR1. The AdipoR1-G269E,G273E mutant transfection inhibited all homodimer and heterodimer formations of AdipoR1 [28]. Therefore, the wild-type AdipoR1 plasmid was first constructed, and Gly269 and Gly273 were subsequently mutated to

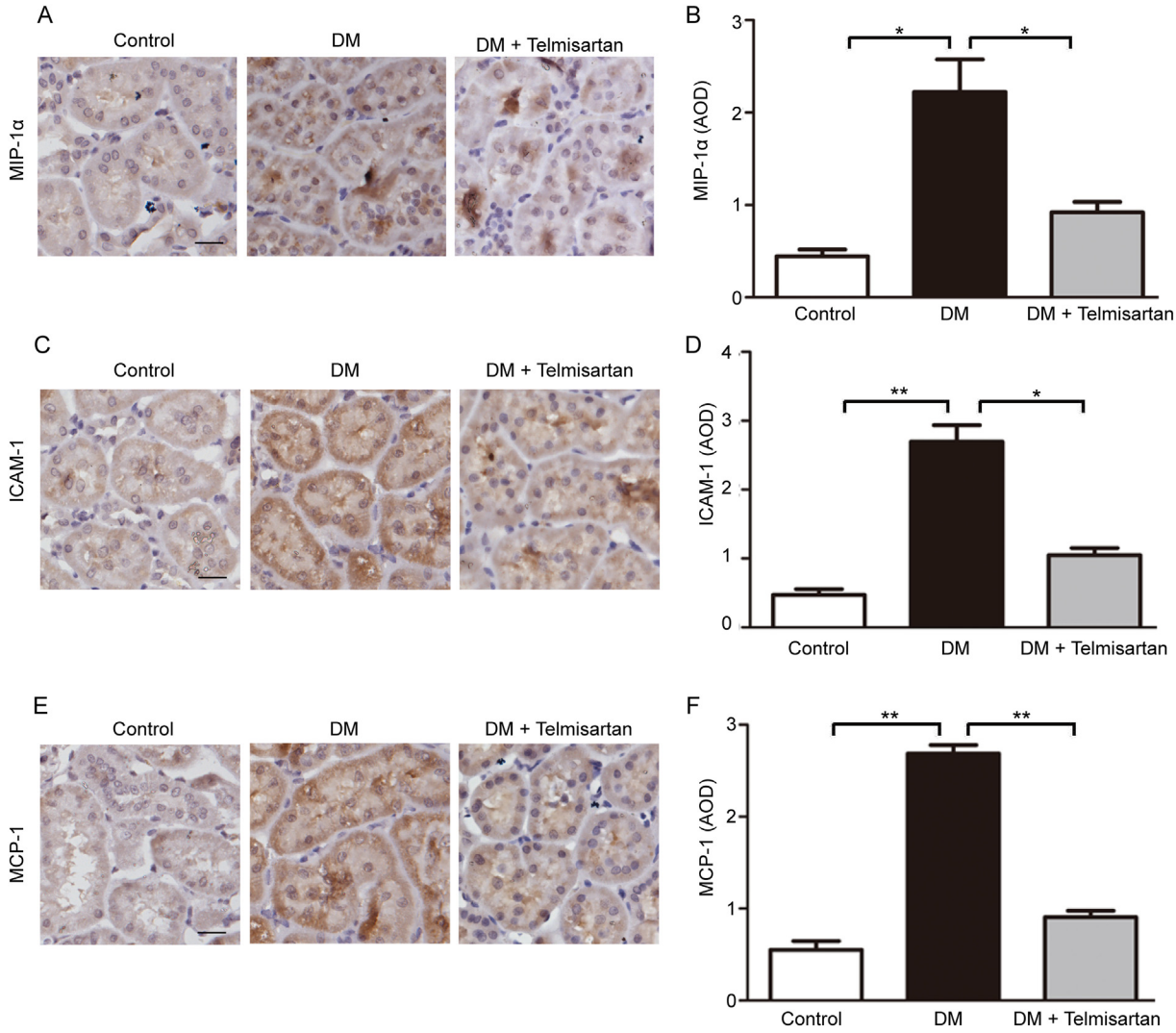

Fig. 5. Telmisartan inhibited the inflammation programming in diabetic kidneys. (A) Representative immunohistochemical staining images, and (B) quantification of the average optical density (AOD) of MIP-1α in kidney sections. (C) ICAM-1 staining and (D) quantification. (E) MCP-1 staining and (F) quantification. Original magnification, ×400; Scale bar = 50 μm; $^{*}P < 0.05$, $^{**}P < 0.001$.

construct the AdipoR1-G269E,G273E mutant. The co-immunoprecipitation analysis revealed that high glucose promoted the dimerization formation of AT1R-AdipoR1 in NRK-52E cells, while AT1R-AdipoR1 heterodimers were almost undetectable in NRK-52E cells transfected with the AdipoR1-G269E,G273E mutant (Fig. 6A–D), suggesting that the AdipoR1-G269E,G273E mutant might facilitate the depolymerization of AT1R-AdipoR1 heterodimers.

Next, the expression of inflammatory factors and fibrotic factors was measured in the absence or presence of AT1R-AdipoR1 dimerization. The western blot results revealed that high glucose instigated the expression of MCP-1, ICAM-1 and NF-κB (Fig. 6E and F), and induced apoptosis in NRK-52E cells (Fig. 6G and H). However, the expression of inflammatory factors, such as MCP-1, ICAM and NF-κB, significantly decreased in NRK-52E cells transfected with the AdipoR1-G269E,G273E mutant (Fig. 6E and F). In addition, transfection with the AdipoR1-G269E,G273E mutant remarkably inhibited the high glucose-induced cell apoptosis in NRK-52E cells (Fig. 6G and H). These results suggest that the high glucose-induced AT1R-AdipoR1 dimerization accelerated the inflammatory response and cell apoptosis in renal tubular epithelial cells, and the depolymerization of AT1R-AdipoR1 heterodimers protected against high glucose-induced renal tubular damage.

3.7. The high glucose-induced heterodimerization of AT1R-AdipoR1 promotes cellular damage through AMPK inactivation in cultured NRK-52E cells

In parallel with the increased heterodimerization of AT1R-AdipoR1 in NRK-52E cells induced by high glucose, the western blot results revealed that high glucose inhibited the activation of AMPK signaling in NRK-52E cells (Fig. 7A and B). In addition, the depolymerization of AT1R-AdipoR1 could restore the expression of p-AMPK in NRK-52E cells exposed to high glucose. In order to analyze the specific signaling of the heterodimerization of AT1R-AdipoR1, NRK-52E cells were treated with 10^{-7} M of angiotensin II for 48 h. It was found that angiotensin II could decrease the expression of AdipoR1 and increase the expression of AT1R in NRK-52E cells (Fig. 7C and D). Interestingly, angiotensin II could not enhance the heterodimerization of AT1R-AdipoR1 (Fig. 7E–H). These results suggest that the high glucose-induced heterodimerization of AT1R-AdipoR1 promoted cellular damage through AMPK inactivation in cultured NRK-52E cells.

3.8. Telmisartan inhibited the dimerization formation of AT1R-AdipoR1 and cellular damage in cultured NRK-52E cells

Confocal microscopy and immunoprecipitation revealed that

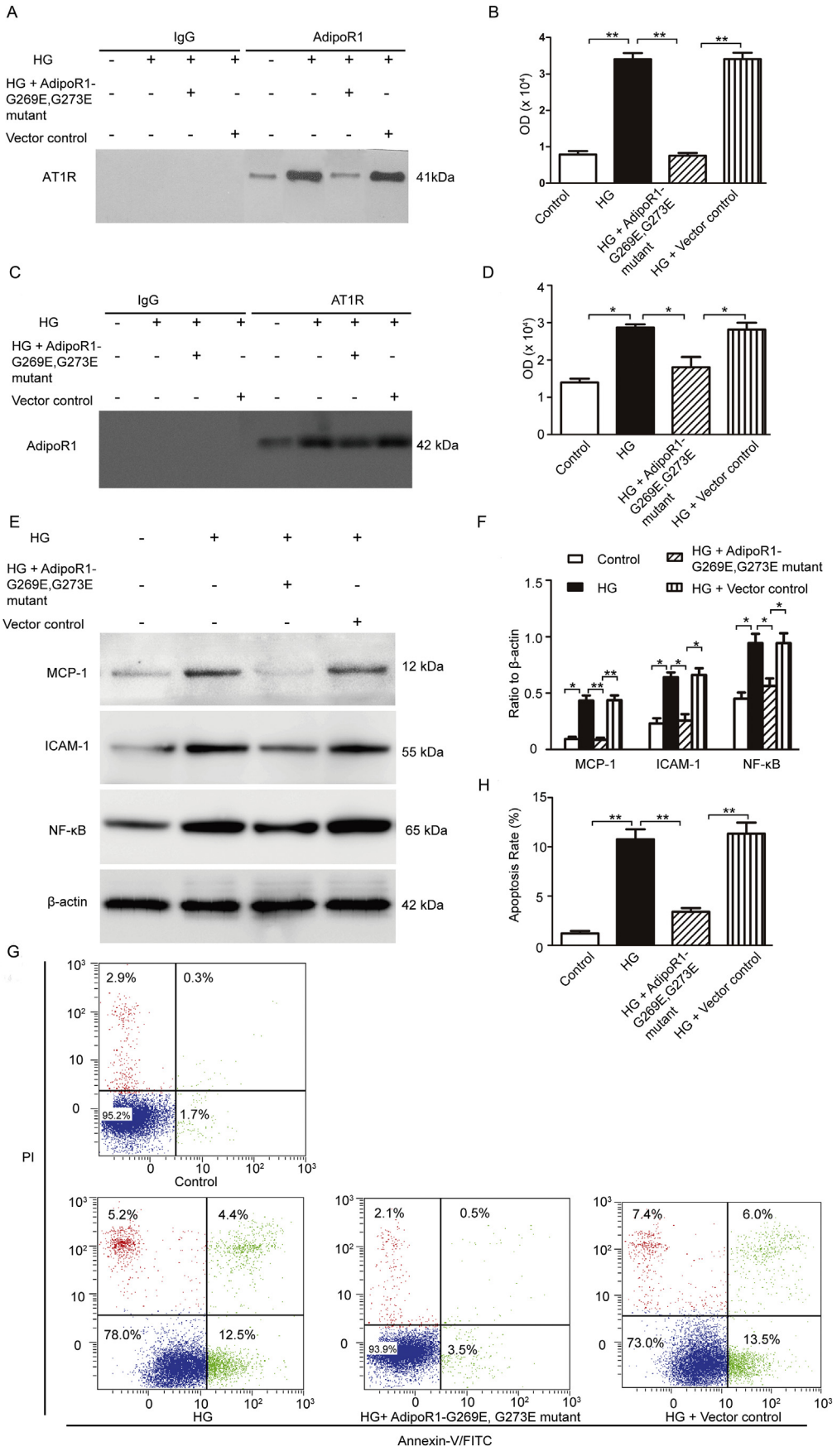

Fig. 6. High glucose-induced heterodimerization of AT1R-AdipoR1 promoted cellular damage in NRK-52E cells. (A–D) The co-immunoprecipitation analysis of AT1R-AdipoR1 heterodimerization in NRK-52E cells treated by high glucose with the AdipoR1-G269E,G273E mutant or control vector transfection (A and C), and the densitometric analysis of the heterodimerization of AT1R-AdipoR1 (B and D). (E) Western blot analysis of the expression of MCP-1, ICAM-1 and NF-κB in NRK-52E cells treated with high glucose, with or without the AdipoR1-G269E,G273E mutant or control vector transfection. (F) Densitometric analysis of MCP-1, ICAM-1 and NF-κB expression normalized with β-actin in the indicated groups. (G) Flow cytometric analysis of apoptosis in NRK-52E cells treated with high glucose, with or without the AdipoR1-G269E,G273E mutant or control vector transfection. (H) Quantitative analysis of apoptosis cells from at least three independent experiments; $^{*}P < 0.05$, $^{**}P < 0.001$.

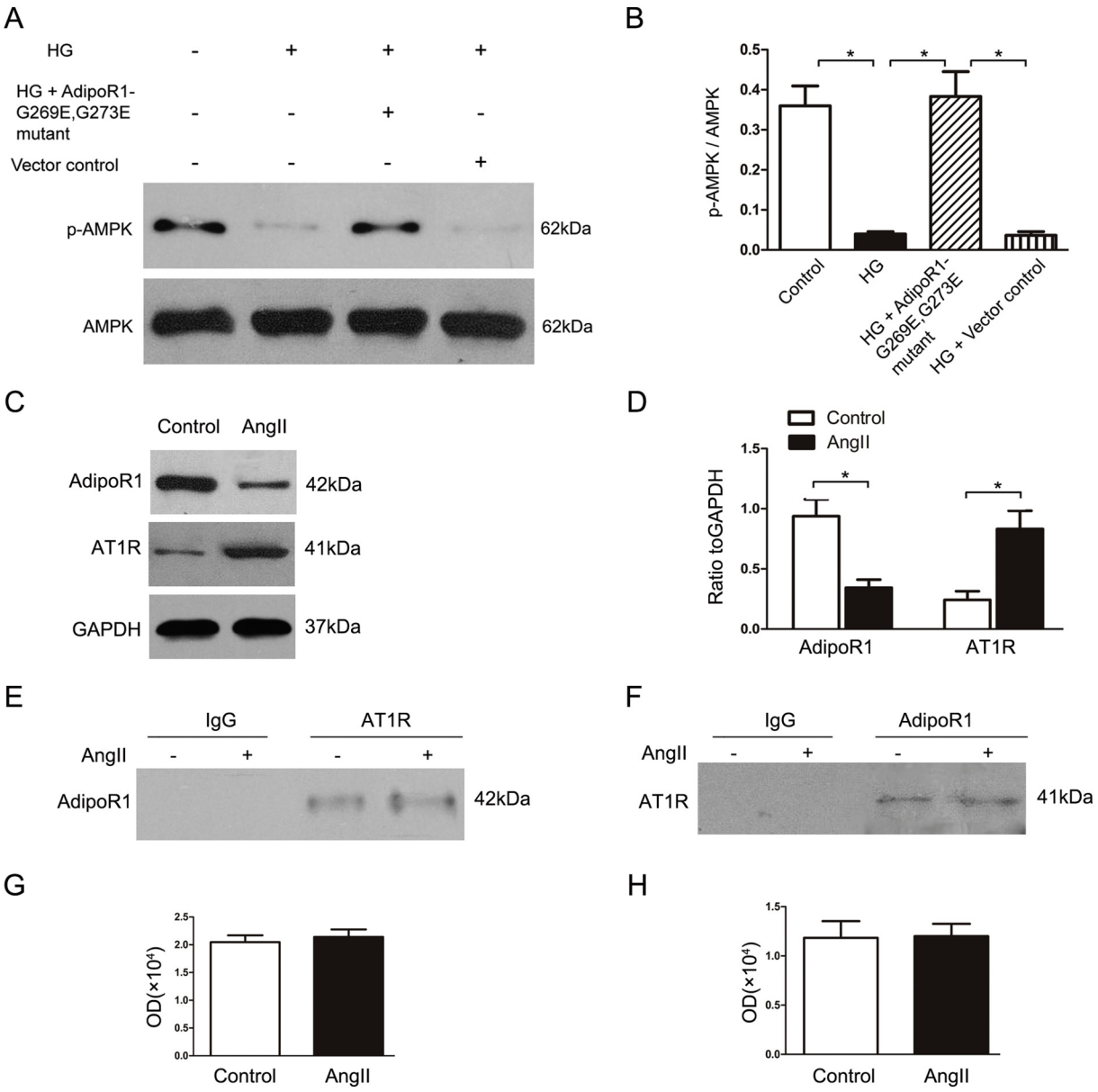

Fig. 7. The high glucose-induced heterodimerization of AT1R-AdipoR1 promoted cellular damage in NRK-52E cells. (A) The western blot analysis of the expression of p-AMPK and AMPK in NRK-52E cells treated with high glucose, with or without the AdipoR1-G269E,G273E mutant or control vector transfection. (B) The densitometric analysis of p-AMPK expression normalized with AMPK in the indicated groups. (C) The western blot analysis of the expression of AdiooR1 and AT1R in NRK-52E cells treated with angiotensin II. (D) The densitometric analysis of AdiooR1 and AT1R expression normalized with β-actin in the indicated groups. (E–H) The co-immunoprecipitation analysis of AT1R-AdipoR1 heterodimerization in NRK-52E cells treated by angiotensin II (E and F), and densitometric analysis of the heterodimerization of AT1R-AdipoR1 (G and H). $^{*}P < 0.05$.

telmisartan inhibited the formation of AT1R-AdipoR1 dimerization induced by high glucose in NRK-52E cells (Fig. 8A–E). These results were proven in another cell line, HK-2 cells, in which immunoprecipitation also revealed the enhanced formation of AT1R-AdipoR1 dimerization induced by high glucose. However, telmisartan diminished the high glucose-induced AT1R-AdipoR1 dimer (Fig. 8F–I).

In paralleled with these results, it was also found that telmisartan suppressed the expression of inflammatory cytokines, such as ICAM-1, NF-κB and MCP-1 (Fig. 8J and K), and alleviated the cell apoptosis induced by high glucose in NRK-52E cells (Fig. 8L and M). Interestingly, the knockdown of AdipoR1 could abate the suppressive effect of telmisartan on inflammatory cytokines, leading to increased expression levels of ICAM-1, NF-κB and MCP-1, when compared with their counterparts in NRK-52E cells (Fig. 8N–O).

4. Discussion

Although several available therapeutic interventions have been reported to retard the progression of DN, morbidity associated with this disease remains high, which raises an urgent need to develop novel and effective therapeutic strategies. The inhibition of renal fibrosis and restoration of normal kidney structure are fundamental processes for exploring therapeutic approaches to combat chronic kidney diseases, including DN [29]. Given that DN is an irreversible and progressive disorder, it is critical to prevent the onset of this disease by targeting specific mechanisms [30,31]. In the present study, telmisartan (5 mg/kg/day) alleviated renal fibrosis and reduced urinary albumin excretion in an experimental rat model of diabetes, and exhibited its renoprotective role in DN independent actions of lowering blood pressure and blood glucose. Although the benefits of telmisartan on DN have

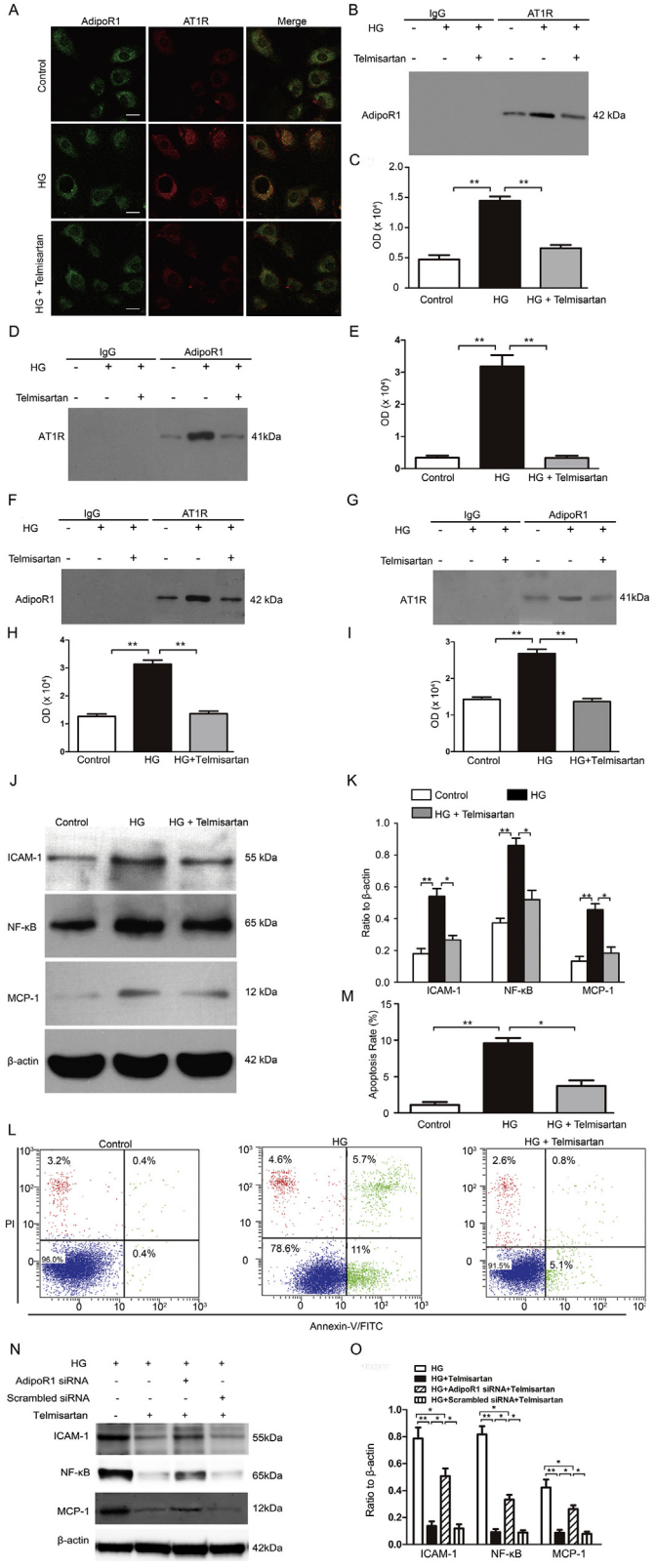

Fig. 8. Telmisartan inhibited the heterodimerization of AdipoR1-AT1R and cellular damage in cultured NRK-52E cells. (A) Representative images of AT1R-AdipoR1 interaction in NRK-52E cells treated with high glucose, with or without telmisartan, by confocal microscopy; Original magnification, ×630; Scale bar = 50 μm. (B–E) The co-immunoprecipitation analysis of AT1R-AdipoR1 interaction in NRK-52E cells treated with high glucose, with or without telmisartan (B and D), and the densitometric analysis of the heterodimerization of AT1R-AdipoR1 (C and E) are presented. (F–I) The co-immunoprecipitation analysis of AT1R-AdipoR1 interaction in HK-2 cells treated with high glucose, with or without telmisartan (F and G), and the densitometric analysis of the heterodimerization of AT1R-AdipoR1 (H and I). (J) The western blot analysis of ICAM-1, NF-κB and MCP-1 expression in NRK-52E cells treated with high glucose, with or without telmisartan. (K) The densitometric analysis of ICAM-1, NF-κB and MCP-1 expression normalized with β-actin in the indicated groups. (L) The flow cytometric analysis of apoptosis in NRK-52E cells treated with high glucose, with or without telmisartan. (M) Quantitative analysis of apoptosis cells from at least three independent experiments. $^{*}P < 0.05$, $^{**}P < 0.001$. (N) Western blot analysis of the expression of ICAM-1, NF-κB and MCP-1 in NRK-52E cells treated with high glucose and telmisartan, with or without AdipoR1 siRNA or control vector transfection. (O) The densitometric analysis of ICAM-1, NF-κB and MCP-1 expression normalized with β-actin in the indicated groups. Data were expressed as mean ± standard error of the mean (SEM); $n = 5$, in each group; $^{*}P < 0.05$, $^{**}P < 0.001$.

been reported [24,32], the underlying mechanisms remain largely unknown. The previous study conducted by the investigators explored the cross-talk interaction between Ang II and adiponectin receptors by detecting the naturally occurring receptor-receptor heterodimerization between AdipoR1 and AT1R, AdipoR1 and AT2R, and AdipoR2 and AT2R [21]. High glucose facilitated the formation of these heterodimers, and resultantly instigated tubulointerstitial injury by inhibiting the cytoprotective actions of adiponectin receptors [21]. These results inspired the investigators to further explore the role of AT1R-AdipoR1 heterodimerization in the pathogenesis of DN, and importantly, the effect of telmisartan on the dimerization formation of AT1R-AdipoR1 during DN.

Normally, adiponectin can bind to its receptor to exert protective effects, such as anti-inflammatory and alleviating insulin resistance [10,13,33,34]. However, serum adiponectin level has been reported to be elevated in type-1 diabetes with or without DN [13,35–37]. In a cross-sectional study, elevated serum adiponectin levels are associated with increased albuminuria and worse renal function in diabetic patients [38]. The above-mentioned evidence suggests that abnormally elevated serum adiponectin may play a role in the development of DN.

In previous *in vitro* experiments conducted by the investigators, AdipoR1 expression remained unchanged in renal tubular epithelial cells after exposure to high glucose. However, high glucose boosted the heterodimers between Ang II receptors and adiponectin receptors, which was in parallel with the upregulation of NF-κB and MCP-1 expression [21]. Consistently, the present study revealed the increase in AT1R-AdipoR1 heterodimers in diabetic kidneys, especially in the renal tubulointerstitial compartment, as well as in renal tubular epithelial cells exposed to high glucose. The enhanced formation of AdipoR1-AT1R dimer was independent of the increased expression of AT1R in cultured NRK-52E cells, indicating that the increase in AdipoR1-AT1R dimer formation was not a result of the change in AT1R protein. It was also found that the inactivation of AMPK in NRK-52E cells exhibited the heterodimerization of AT1R-AdipoR1 under high glucose conditions. In contrast, the depolymerization of AT1R-AdipoR1 could restore the expression of p-AMPK in NRK-52E cells. A defect in AMPK function has been found in a variety of metabolic diseases [39–42]. In obesity and diabetes, AMPK activation is compromised, which may trigger the proinflammatory response and exacerbate the disease condition [41]. These evidences suggest that the high glucose-induced heterodimerization of AT1R-AdipoR1 promoted cellular damage probably through AMPK inactivation, but this still needs to be further investigated.

In parallel with higher serum adiponectin and the unchanged AdipoR1 expression, diabetic rats displayed increased inflammatory cytokines in the renal tubulointerstitial compartment [21]. These findings reveal the existence of adiponectin resistance in diabetic renal tubular epithelial cells. Given the prominent role of inflammation in the

pathogenesis of DN *via* the recruitment of proinflammatory cytokines, the effect of AT1R-AdipoR1 dimerization in the DN model has been speculated to be associated with inflammation [43–45].

In order to investigate the effect of AT1R-AdipoR1 heterodimerization on DN, AT1R-AdipoR1 heterodimers were depolymerized *via* the AdipoR1-G269E,G273E mutant transfection *in vitro* [28]. It was found that the depolymerization of AT1R-AdipoR1 heterodimers alleviated high glucose-induced inflammation and cell apoptosis in renal tubular epithelial cells, suggesting that AT1R-AdipoR1 heterodimerization was involved in the progression of DN through mediating inflammatory response and inducing cell apoptosis.

Taken together, the investigators boldly hypothesized that AT1R-AdipoR1 heterodimerization might be involved in the development of DN. The heterodimerization of AT1R-AdipoR1 was significantly increased in diabetic kidneys, or in renal tubular epithelial cells exposed to high glucose. As a consequence, dissociative AdipoR1 was reduced. This was accompanied by decreased binding sites of AdipoR1 for adiponectin, which led to adiponectin resistance and the dysfunction of adiponectin signaling. Although the expression of AdipoR1 remained unchanged in the diabetic tubular compartment, AdipoR1 engaged in the heterodimerization of AT1R-AdipoR1, instead of adiponectin signaling. This instigated tubulointerstitial injury through inflammatory response and cell apoptosis. However, this deduction was not conclusive, and needs further confirmation.

The present results of the diabetic rat model revealed that telmisartan inhibited the heterodimerization of AT1R-AdipoR1 in kidneys, particularly in the renal tubular compartment. Consistently, the *in vitro* results were proven in NRK-52E cells, as well as in HK-2 cells, in which immunoprecipitation revealed the enhanced formation of AT1R-AdipoR1 dimerization induced by high glucose. However, telmisartan could diminish the high glucose-induced AT1R-AdipoR1 dimer. It was also found that telmisartan inhibited inflammatory cytokines in the diabetic tubulointerstitial compartment, as well as high glucose-induced apoptosis in renal tubular epithelial cells. These results indicate that the renoprotective effect of telmisartan may be associated to its capacity to inhibit AT1R-AdipoR1 heterodimerization, and alleviate downstream inflammatory responses and cell apoptosis. Further research was performed to determine whether the absence of AdipoR1 could attenuate the renoprotective benefits of telmisartan. The *in vitro* and *in vivo* data revealed that AdipoR1 knockdown could abate the renoprotective role of telmisartan, which further supports the link between the benefits of telmisartan and its inhibitory effect on AT1R-AdipoR1 heterodimerization.

5. Conclusion

The present study demonstrated that the heterodimerization of AT1R-AdipoR1 promoted inflammatory response and cell apoptosis in the renal tubular compartment during the progression of DN. In addition, telmisartan attenuated the renal damage of DN through the inhibition of AT1R-AdipoR1 heterodimerization, and alleviation of downstream inflammatory responses and cell apoptosis. The present study may provide a novel mechanism underlying the renoprotective effect of telmisartan in the treatment of DN.

Acknowledgements

This work was supported in part by the National Science Foundation of China (81400694 to D. Zha and 81170679 to X. Wu).

Conflict of interest statement

The authors declare that there are no conflicts of interest in this work.

References

[1] KDOQI Clinical practice guidelines and clinical practice recommendations for diabetes and chronic kidney disease, Am. J. Kidney Dis. 49 (2007) S12–154.
[2] I.H. de Boer, T.C. Rue, Y.N. Hall, P.J. Heagerty, N.S. Weiss, J. Himmelfarb, Temporal trends in the prevalence of diabetic kidney disease in the United States, JAMA 305 (2011) 2532–2539.
[3] A. Takahashi, Y. Takabatake, T. Kimura, I. Maejima, T. Namba, T. Yamamoto, J. Matsuda, S. Minami, J.Y. Kaimori, I. Matsui, T. Matsusaka, F. Niimura, T. Yoshimori, Y. Isaka, Autophagy inhibits the accumulation of advanced glycation end products by promoting lysosomal biogenesis and function in the kidney proximal tubules, Diabetes 66 (2017) 1359–1372.
[4] N.A. El-Mahdy, M.E. El-Sayad, A.H. El-Kadem, Combination of telmisartan with sildenafil ameliorate progression of diabetic nephropathy in streptozotocin-induced diabetic model, Biomed. Pharmacother. 81 (2016) 136–144.
[5] H. Noh, G.L. King, The role of protein kinase C activation in diabetic nephropathy, Kidney Int. Suppl. (2007) S49–S53.
[6] Z. Lu, N. Liu, Epigenetic regulations in diabetic nephropathy, 2017 (2017) 7805058.
[7] E. Feigerlova, S.F. Battaglia-Hsu, IL-6 signaling in diabetic nephropathy: from pathophysiology to therapeutic perspectives, Cytokine Growth Factor Rev. 37 (2017) 57–65.
[8] L. Lieben, Diabetic nephropathy: lipid toxicity drives renal disease, Nat. Rev. Nephrol. 13 (2017) 194.
[9] Z. Ilyas, J.T. Chaiban, A. Krikorian, Novel insights into the pathophysiology and clinical aspects of diabetic nephropathy, 18 (2017) 21–28.
[10] T. Yamauchi, J. Kamon, Y. Ito, A. Tsuchida, T. Yokomizo, S. Kita, T. Sugiyama, M. Miyagishi, K. Hara, M. Tsunoda, K. Murakami, T. Ohteki, S. Uchida, S. Takekawa, H. Waki, N.H. Tsuno, Y. Shibata, Y. Terauchi, P. Froguel, K. Tobe, S. Koyasu, K. Taira, T. Kitamura, T. Shimizu, R. Nagai, T. Kadowaki, Cloning of adiponectin receptors that mediate antidiabetic metabolic effects, Nature 423 (2003) 762–769.
[11] W.L. Holland, J.Y. Xia, J.A. Johnson, K. Sun, M.J. Pearson, A.X. Sharma, E. Quittner-Strom, T.S. Tippetts, R. Gordillo, P.E. Scherer, Inducible overexpression of adiponectin receptors highlight the roles of adiponectin-induced ceramidase signaling in lipid and glucose homeostasis, Mol. Metab. 6 (2017) 267–275.
[12] G.A. Christou, D.N. Kiortsis, The role of adiponectin in renal physiology and development of albuminuria, J. Endocrinol. 221 (2014) R49–R61.
[13] D. Zha, X. Wu, P. Gao, Adiponectin and its receptors in diabetic kidney disease: molecular mechanisms and clinical potential, Endocrinology 158 (2017) 2022–2034.
[14] Y. Kim, J.H. Lim, M.Y. Kim, E.N. Kim, H.E. Yoon, S.J. Shin, B.S. Choi, Y.S. Kim, Y.S. Chang, C.W. Park, The adiponectin receptor agonist AdipoRon ameliorates diabetic nephropathy in a model of type 2 diabetes, J. Am. Soc. Nephrol. 29 (2018) 1108–1127.
[15] C.M. van Stijn, J. Kim, G.D. Barish, U.J. Tietge, R.K. Tangirala, Adiponectin expression protects against angiotensin II-mediated inflammation and accelerated atherosclerosis, PLoS One 9 (2014) e86404.
[16] F. Fang, G.C. Liu, C. Kim, R. Yassa, J. Zhou, J.W. Scholey, Adiponectin attenuates angiotensin II-induced oxidative stress in renal tubular cells through AMPK and cAMP-Epac signal transduction pathways, Am. J. Physiol. Ren. Physiol. 304 (2013) F1366–F1374.
[17] C. Lyngso, N. Erikstrup, J.L. Hansen, Functional interactions between 7TM receptors in the renin-angiotensin system—dimerization or crosstalk? Mol. Cell. Endocrinol. 302 (2009) 203–212.
[18] M. Audet, M. Bouvier, Restructuring G-protein- coupled receptor activation, Cell 151 (2012) 14–23.
[19] G.E. Breitwieser, G protein-coupled receptor oligomerization: implications for G protein activation and cell signaling, Circ. Res. 94 (2004) 17–27.
[20] S. AbdAlla, H. Lother, A. Langer, Y. el Faramawy, U. Quitterer, Factor XIIIA transglutaminase crosslinks AT1 receptor dimers of monocytes at the onset of atherosclerosis, Cell 119 (2004) 343–354.
[21] D. Zha, H. Cheng, W. Li, Y. Wu, X. Li, L. Zhang, Y.H. Feng, X. Wu, High glucose instigates tubulointerstitial injury by stimulating hetero-dimerization of adiponectin and angiotensin II receptors, Biochem. Biophys. Res. Commun. 493 (2017) 840–846.
[22] O. Tsuprykov, R. Ando, C. Reichetzeder, K. von Websky, V. Antonenko, Y. Sharkovska, L. Chaykovska, J. Rahnenfuhrer, A.A. Hasan, H. Tammen, M. Alter, T. Klein, S. Ueda, S.I. Yamagishi, S. Okuda, B. Hocher, The dipeptidyl peptidase inhibitor linagliptin and the angiotensin II receptor blocker telmisartan show renal benefit by different pathways in rats with 5/6 nephrectomy, Kidney Int. 89 (2016) 1049–1061.
[23] C. Sato-Horiguchi, D. Ogawa, J. Wada, H. Tachibana, R. Kodera, J. Eguchi, A. Nakatsuka, N. Terami, K. Shikata, H. Makino, Telmisartan attenuates diabetic nephropathy by suppressing oxidative stress in db/db mice, Nephron Exp. Nephrol. 121 (2012) e97–e108.
[24] P. Balakumar, H. K. Bishnoi, N. Mahadevan, Telmisartan in the management of diabetic nephropathy: a contemporary view, Curr. Diabetes Rev. 8 (2012) 183–190.
[25] L. Li, Z.G. Zhang, H. Lei, C. Wang, L.P. Wu, J.Y. Wang, F.Y. Fu, W.G. Zhu, L.L. Wu, Angiotensin II reduces cardiac AdipoR1 expression through AT1 receptor/ROS/ERK1/2/c-Myc pathway, PLoS One 8 (2013) e49915.
[26] Z. Guo, C. Zheng, Z. Qin, P. Wei, Effect of telmisartan on the expression of cardiac adiponectin and its receptor 1 in type 2 diabetic rats, J. Pharm. Pharmacol. 63 (2011) 87–94.
[27] National Research Council (US) Committee for the Update of the Guide for the Care

and Use of Laboratory Animals, Guide for the Care and Use of Laboratory Animals, 8th edition, National Academies Press (US), Washington (DC), 2011.
[28] D. Kosel, J.T. Heiker, C. Juhl, C.M. Wottawah, M. Bluher, K. Morl, A.G. Beck-Sickinger, Dimerization of adiponectin receptor 1 is inhibited by adiponectin, J. Cell Sci. 123 (2010) 1320–1328.
[29] K. Kanasaki, S. Shi, M. Kanasaki, J. He, T. Nagai, Y. Nakamura, Y. Ishigaki, M. Kitada, S.P. Srivastava, D. Koya, Linagliptin-mediated DPP-4 inhibition ameliorates kidney fibrosis in streptozotocin-induced diabetic mice by inhibiting endothelial-to-mesenchymal transition in a therapeutic regimen, Diabetes 63 (2014) 2120–2131.
[30] B. Quiroga, D. Arroyo, Present and future in the treatment of diabetic kidney disease, 2015 (2015) 801348.
[31] J. Himmelfarb, K.R. Tuttle, New therapies for diabetic kidney disease, N. Engl. J. Med. 369 (2013) 2549–2550.
[32] R.E. Schmieder, G. Bakris, M.R. Weir, Telmisartan in incipient and overt diabetic renal disease, J. Nephrol. 24 (2011) 263–273.
[33] H. Ruan, L.Q. Dong, Adiponectin signaling and function in insulin target tissues, J. Mol. Cell Biol. 8 (2016) 101–109.
[34] T. Kadowaki, T. Yamauchi, N. Kubota, K. Hara, K. Ueki, K. Tobe, Adiponectin and adiponectin receptors in insulin resistance, diabetes, and the metabolic syndrome, J. Clin. Invest. 116 (2006) 1784–1792.
[35] A. Jorsal, L. Tarnow, J. Frystyk, M. Lajer, A. Flyvbjerg, H.H. Parving, N. Vionnet, P. Rossing, Serum adiponectin predicts all-cause mortality and end stage renal disease in patients with type I diabetes and diabetic nephropathy, Kidney Int. 74 (2008) 649–654.
[36] T.P. Combs, J.K. Snell-Bergeon, D.M. Maahs, B.C. Bergman, M. Lamarche, L. Iberkleid, O. AbdelBaky, R. Tisch, P.E. Scherer, E.B. Marliss, Adiponectin-SOGA dissociation in type 1 diabetes, J. Clin. Endocrinol. Metab. 100 (2015) E1065–E1073.
[37] P. Bjornstad, L. Pyle, G.L. Kinney, M. Rewers, R.J. Johnson, D.M. Maahs, J.K. Snell-Bergeon, Adiponectin is associated with early diabetic kidney disease in adults with type 1 diabetes: a Coronary Artery Calcification in Type 1 Diabetes (CACTI) Study, J. Diabetes Complicat. 31 (2017) 369–374.
[38] H.C. Looker, J. Krakoff, T. Funahashi, Y. Matsuzawa, S. Tanaka, R.G. Nelson, W.C. Knowler, R.S. Lindsay, R.L. Hanson, Adiponectin concentrations are influenced by renal function and diabetes duration in Pima Indians with type 2 diabetes, J. Clin. Endocrinol. Metab. 89 (2004) 4010–4017.
[39] K.A. Coughlan, R.J. Valentine, N.B. Ruderman, A.K. Saha, AMPK activation: a therapeutic target for type 2 diabetes? Diab. Metab. Syndr. Obes. 7 (2014) 241–253.
[40] B. Viollet, F. Andreelli, AMP-activated protein kinase and metabolic control, Handb. Exp. Pharmacol. (2011) 303–330.
[41] B. Viollet, S. Horman, J. Leclerc, L. Lantier, M. Foretz, M. Billaud, S. Giri, F. Andreelli, AMPK inhibition in health and disease, Crit. Rev. Biochem. Mol. Biol. 45 (2010) 276–295.
[42] S.M. Jeon, Regulation and function of AMPK in physiology and diseases, Exp. Mol. Med. 48 (2016) e245.
[43] J. Donate-Correa, E. Martin-Nunez, M. Muros-de-Fuentes, C. Mora-Fernandez, J.F. Navarro-Gonzalez, Inflammatory cytokines in diabetic nephropathy, J. Diabetes Res. 2015 (2015) 948417.
[44] J.F. Navarro-Gonzalez, C. Mora-Fernandez, The role of inflammatory cytokines in diabetic nephropathy, J. Am. Soc. Nephrol. 19 (2008) 433–442.
[45] J.F. Navarro-Gonzalez, C. Mora-Fernandez, M. Muros de Fuentes, J. Garcia-Perez, Inflammatory molecules and pathways in the pathogenesis of diabetic nephropathy, Nat. Rev. Nephrol. 7 (2011) 327–340.